Soft Matter

Van't Hoff's law for active suspensions: the role of the solvent chemical potential†
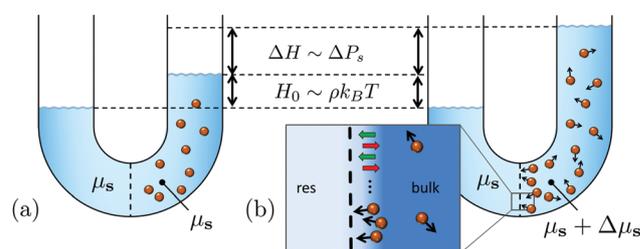
Jeroen Rodenburg, [ID] [a] Marjolein Dijkstra[b] and René van Roij[a]

We extend Van't Hoff's law for the osmotic pressure to a suspension of active Brownian particles. The propelled particles exert a net reaction force on the solvent, and thereby either drive a measurable solvent flow from the connecting solvent reservoir through the semipermeable membrane, or increase the osmotic pressure and cause the suspension to rise to heights as large as micrometers for experimentally realized microswimmers described in the literature. The increase in osmotic pressure is caused by the background solvent being, in contrast to passive suspensions, no longer at the chemical potential of the solvent reservoir. The difference in solvent chemical potentials depends on the colloid–membrane interaction potential, which implies that the osmotic pressure is a state function of a state that *itself* is influenced by the membrane potential.

Introduction

In 1887, Van't Hoff formulated his famous law stating that the osmotic pressure Π of a dilute suspension equals the pressure $\rho k_B T$ of a dilute gas of the same concentration ρ and temperature T, with k_B the Boltzmann constant.[1–3] In Van't Hoff's interpretation, the total pressure of the suspension $P_{\text{tot}}(\rho,\mu_s) = \rho k_B T + P_s(\mu_s)$ decomposes into the sum of the effective colloid-only pressure $\rho k_B T$ and a 'background' pressure $P_s(\mu_s)$ of the solvent at chemical potential μ_s. In the typical experimental setup to measure osmotic pressure (Fig. 1), μ_s is set by a solvent reservoir that connects to the suspension *via* a membrane permeable to solvent only. The net force per unit area exerted on the membrane defines the osmotic pressure, and results from the difference in suspension pressure $P_{\text{tot}}(\rho,\mu_s)$ and reservoir pressure $P_s(\mu_s)$. As this pressure difference induces a height difference H between the two menisci, the osmotic pressure $\Pi \sim H$ can be directly inferred.

Van't Hoff's law does not apply to non-equilibrium suspensions of active particles that constantly convert energy into directed motion, such as swimming bacteria[4,5] or artificial microswimmers.[6] Not only are these systems promising for applications in *e.g.* self-assembly[7,8] and targeted cargo transport,[9,10] they also display remarkable phase behaviour[11–20] that calls for an underpinning thermodynamic framework.[21–32] An essential

Fig. 1 Schematic setup to measure osmotic pressure Π from the height difference $H = H_0 + \Delta H$ between the two menisci. (a) For a passive system, the solvent chemical potential of the suspension equals the reservoir chemical potential μ_s, such that $\Pi = \rho k_B T$ and $H = H_0 \sim \rho k_B T$. (b) For an active system, colloids tend to 'propel into' the membrane (green arrows), thereby exerting the opposite reaction force on the solvent (red arrows). As a result, the solvent pressure and solvent chemical potential in the bulk suspension increase by ΔP_s and $\Delta \mu_s$, respectively, indicated by the darker blue background, such that Π and H increase by ΔP_s and $\Delta H \sim \Delta P_s$, respectively.

prerequisite for such a framework is that thermodynamic properties can be expressed as functions of variables that characterize the system state, a seemingly trivial condition that was nonetheless questioned for the osmotic pressure.[33]
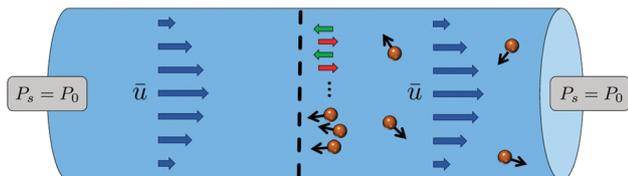
Previous studies of the pressure[33–54] mostly addressed self-propelled particles on a substrate, or equivalently, an effective colloid-only system without an explicit solvent. The solvent *was* explicitly modelled in ref. 55, but only as a passive species unaffected by the propulsion force. However, as the propulsion force is internal,[56] the solvent – and in particular its pressure – *is* affected by the opposite reaction force.[41]

In this work, we apply this insight to extend Van't Hoff's law to active suspensions. We show the osmotic pressure to increase with activity due to a difference in *solvent* pressure that

a Institute for Theoretical Physics, Center for Extreme Matter and Emergent Phenomena, Utrecht University, Princetonplein 5, 3584 CC Utrecht, The Netherlands. E-mail: a.j.rodenburg@uu.nl, r.vanroij@uu.nl

b Soft Condensed Matter Group, Debye Institute for Nanomaterials Science, Utrecht University, Princetonplein 5, 3584 CC Utrecht, The Netherlands

Fig. 2 Schematic setup to measure how active colloids confined to one side of a semipermeable membrane in an open pipe affect the solvent, viewed in the lab frame. As the colloids tend to 'propel into' the membrane (green arrows), they exert the opposite reaction force on the solvent (red arrows). Under boundary conditions of equal solvent pressure P_s on either side of the pipe, the reaction force drives a parabolic solvent flow profile of mean velocity $\bar{u}$, as indicated by the blue arrows.

develops between the suspension and the reservoir. The effect of this solvent pressure difference is predicted to be experimentally measurable, either as an additional meniscus rise ΔH (Fig. 1), or as a solvent flow through a semipermeable membrane towards the active particles in an open system (Fig. 2). The solvent pressure difference implies also a difference in solvent chemical potential, that, remarkably, depends on the details of the colloid–membrane interactions. We will conclude that the osmotic pressure *is* a state function of a state that *itself*, however, is affected by the colloid–membrane interaction potential.

Model

We model the effective one-component system of suspended particles as overdamped active Brownian particles (ABPs).[12,57] Every particle is characterized by a three-dimensional position $\mathbf{r}$ and an orientation $\hat{\mathbf{e}}$. It is well known that the probability density $\psi(\mathbf{r},\hat{\mathbf{e}},t)$ satisfies the Smoluchowski equation (see Section 1 of the ESI†)

$$\partial_t \psi(\mathbf{r},\hat{\mathbf{e}},t) = -\nabla \cdot \mathbf{j}(\mathbf{r},\hat{\mathbf{e}},t) - \nabla_{\hat{\mathbf{e}}} \cdot \mathbf{j}_{\hat{\mathbf{e}}}(\mathbf{r},\hat{\mathbf{e}},t), \qquad (1)$$

and that the translational flux $\mathbf{j}$ and rotational flux $\mathbf{j}_{\hat{\mathbf{e}}}$ follow from the force and torque balance,

$$\begin{aligned}
0 &= -\gamma_t \mathbf{j} - \psi \nabla V(\mathbf{r},\hat{\mathbf{e}}) + \gamma_t v_0 \psi \hat{\mathbf{e}} - k_B T \nabla \psi \quad \text{and} \\
0 &= -\gamma_r \mathbf{j}_{\hat{\mathbf{e}}} - \psi \nabla_{\hat{\mathbf{e}}} V(\mathbf{r},\hat{\mathbf{e}}) - k_B T \nabla_{\hat{\mathbf{e}}} \psi,
\end{aligned} \qquad (2)$$

respectively, between (i) the frictional force and torque, with friction coefficients γ_t and γ_r, (ii) an external force and torque generated by the external potential $V(\mathbf{r},\hat{\mathbf{e}})$ acting on every particle, (iii) a constant self-propulsion force, corresponding to propulsion speed v_0, acting along each particle's orientation $\hat{\mathbf{e}}$, and (iv) Brownian forces and torques giving rise to translational and rotational diffusion. In order to focus on the essential physics, we follow Van't Hoff and consider the dilute limit, where effective colloid–colloid interactions can be ignored, and where also hydrodynamic interactions are expected to be nonessential. Furthermore, we assume a steady state, *i.e.* $\partial_t \psi = 0$. We analyse the force balance by taking the zeroth moment of eqn (2), which upon defining the density $\rho(\mathbf{r}) \equiv \int d\hat{\mathbf{e}} \psi(\mathbf{r},\hat{\mathbf{e}})$, the polarization $\mathbf{m}(\mathbf{r}) \equiv \int d\hat{\mathbf{e}} \psi(\mathbf{r},\hat{\mathbf{e}})\hat{\mathbf{e}}$, and the colloid flux $\mathbf{J}(\mathbf{r}) \equiv \int d\hat{\mathbf{e}} \mathbf{j}(\mathbf{r},\hat{\mathbf{e}})$, yields

the balance

$$\begin{aligned}
0 &= -\gamma_t \mathbf{J}(\mathbf{r}) - \int d\hat{\mathbf{e}} \psi \nabla V(\mathbf{r},\hat{\mathbf{e}}) + \gamma_t v_0 \mathbf{m}(\mathbf{r}) - k_B T \nabla \rho(\mathbf{r}) \\
&\equiv \mathbf{f}^f(\mathbf{r}) + \mathbf{f}^e(\mathbf{r}) + \mathbf{f}^p(\mathbf{r}) - \nabla P(\mathbf{r})
\end{aligned} \qquad (3)$$

between the frictional body force $\mathbf{f}^f$, the external body force $\mathbf{f}^e$, the propulsion body force $\mathbf{f}^p$, and the pressure gradient force $-\nabla P$. The form of the propulsion body force,

$$\mathbf{f}^p(\mathbf{r}) \equiv \gamma_t v_0 \mathbf{m}(\mathbf{r}), \qquad (4)$$

is easily understood as the sum of propulsion forces $\gamma_t v_0 \hat{\mathbf{e}}$ acting on individual colloids. Just like the frictional force $\mathbf{f}^f$, the propulsion force $\mathbf{f}^p$ is an *internal* force.

We now turn our attention to the solvent, that we assume to be incompressible and at small Reynolds number. On a scale coarse-grained over the colloids – *i.e.* the same scale eqn (3) applies to – the local solvent velocity $\mathbf{u}(\mathbf{r})$ is governed by the Stokes equation

$$\mathbf{f}_e^s(\mathbf{r}) - \mathbf{f}^f(\mathbf{r}) - \mathbf{f}^p(\mathbf{r}) - \nabla P_s(\mathbf{r}) + \eta \nabla^2 \mathbf{u}(\mathbf{r}) = 0, \qquad (5)$$

as derived in Section 2 of the ESI.† Eqn (5) is simply the solvent force balance equipped with a possible external body force $\mathbf{f}_s^e(\mathbf{r})$, and the opposite internal body forces $-\mathbf{f}^f(\mathbf{r})$ and $-\mathbf{f}^p(\mathbf{r})$ as reaction forces, in accordance with Newton's third law. Furthermore, $P_s(\mathbf{r})$ is the solvent pressure, and η the dynamic viscosity.

Osmotic pressure

To represent the setting of Fig. 1, we assume an external potential due to a semipermeable membrane that is planar and normal to the Cartesian unit vector $\hat{\mathbf{z}}$, *i.e.* $V(\mathbf{r},\hat{\mathbf{e}}) = V(z,\theta)$, with $\cos\theta \equiv \hat{\mathbf{e}}\cdot\hat{\mathbf{z}}$. This implies $\psi(\mathbf{r},\hat{\mathbf{e}}) = \psi(z,\theta)$, $\mathbf{J}(\mathbf{r}) = J_z(z)\hat{\mathbf{z}}$ *etc*. The potential $V(z,\theta)$ is assumed to decay from ∞ in an infinitely large reservoir, located at $z < 0$ and containing z-coordinate $z_{res} \ll 0$ in bulk, to 0 in the suspension, located at $z > 0$ and containing $z_b \gg 0$ in bulk. The zeroth moment of eqn (1), $\partial_z J_z(z) = 0$, together with a no-flux boundary condition, then implies $J_z(z) = 0$, and hence the frictional body force $\mathbf{f}^f(z) = 0$. For a state without any solvent flow ($\mathbf{u} = 0$), and for a membrane perfectly invisible to the solvent ($\mathbf{f}_s^e = 0$), eqn (5) then simplifies to $-f_z^p(z) - \partial_z P_s(z) = 0$.

For a passive system, where the propulsion body force $f_z^p(z) = 0$, this solvent force balance guarantees equal solvent pressures in the bulk suspension and solvent reservoir, *i.e.* $\Delta P_s \equiv P_s(z_b) - P_s(z_{res}) = 0$. In an active system, however, the existence of a nonzero propulsion force $f_z^p(z)$ results in a difference in these solvent pressures, derived in Section 4 of the ESI† to be

$$\begin{aligned}
\Delta P_s &= -\int_{z_{res}}^{z_b} dz\, f_z^p(z) \\
&= \frac{\gamma_t \gamma_r v_0^2}{6 k_B T} \rho - \frac{\gamma_t v_0}{2 k_B T} \int_{z_{res}}^{z_b} dz \int d\hat{\mathbf{e}} \psi(z,\theta) \sin(\theta) \partial_\theta V(z,\theta).
\end{aligned} \qquad (6)$$

The first term on the right-hand side of eqn (6) corresponds to what is known as the swim pressure,[34,36,42] which we thus

actually identify as a difference in solvent pressure. The second term on the right-hand side of eqn (6), present for particles experiencing a torque $-\partial_\theta V(z,\theta)$, is of special interest because it leads to the conclusion that ΔP_s depends on the potential $V(z,\theta)$. This issue will be discussed later.

The force balance of the total suspension simply follows as the sum of the colloid force balance (3) and the solvent force balance (5), yielding in the planar and flow-free geometry of interest
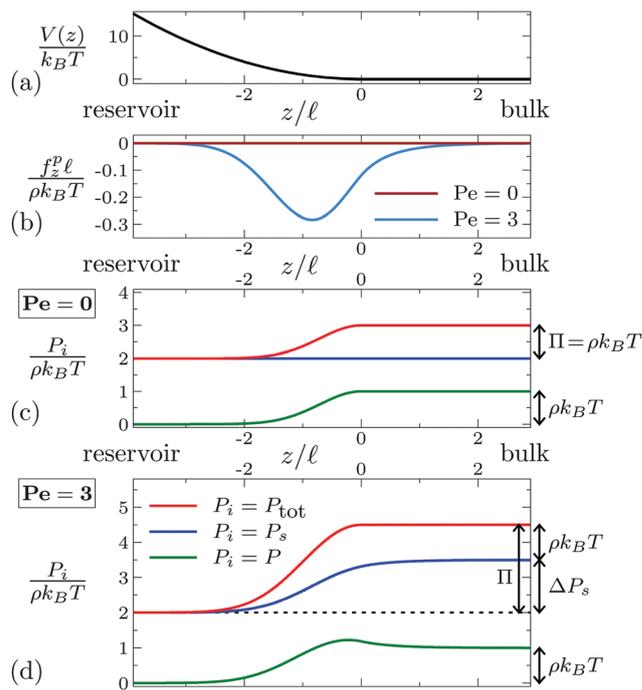
$$f_z^e(z) - \partial_z P_{tot}(z) = 0, \qquad (7)$$

where $P_{tot}(z) \equiv P(z) + P_s(z)$. From the total force balance (7), the osmotic pressure $\Pi \equiv \int_{z_{res}}^{z_b} dz f_z^e(z)$, defined as the magnitude of the force per unit area exerted on the membrane, follows as $P_{tot}(z_b) - P_s(z_{res})$. As the total bulk pressure decomposes into colloid and solvent contributions as $P_{tot}(z_b) = \rho k_B T + P_s(z_b)$, the osmotic pressure reads

$$\Pi = \rho k_B T + \Delta P_s. \qquad (8)$$

In equilibrium, eqn (8) reduces to Van't Hoff's result $\Pi = \rho k_B T$ on account of $\Delta P_s = 0$. Activity increases the osmotic pressure by increasing the solvent pressure with respect to the reservoir by ΔP_s, which is the key result of this work. Together, eqn (8) and (6) generalize Van't Hoff's law to active suspensions.

To clarify these concepts further, we have solved the Smoluchowski eqn (1) numerically for a system of spheres subject to a propulsion force, characterized by Peclet number $Pe \equiv (\gamma_t \gamma_r)^{1/2} v_0 / k_B T$, in the planar geometry modelling the setting of Fig. 1. The membrane, felt by the colloids only, is modelled by the soft potential $V(z) = \lambda k_B T (z/\ell)^2$ for $z < 0$ and $V(z) = 0$ for $z \geq 0$ (Fig. 3(a)), i.e. there is no torque. Here $\lambda = 1$ is the strength of the potential, and $\ell \equiv (\gamma_r/\gamma_t)^{1/2}$ is the appropriate unit of length, which is of the order of the (effective) particle size upon using Stokes relations for γ_t and γ_r. Fig. 3(b) shows the profile of the propulsion body force $f_z^p(z)$. Whereas $f_z^p(z) = 0$ for a passive system ($Pe = 0$), an active system displays a nonzero polarization $m_z(z)$, and thus by eqn (4) a propulsion body force $f_z^p(z)$, in the vicinity of the membrane directed towards the membrane. This well-known effect[58-63] is in this case caused by colloids persistently propelling 'into' the repulsive membrane. Fig. 3(c), for $Pe = 0$, shows the pressure profiles $P(z)$ of the passive colloids, $P_s(z)$ of the solvent, and $P_{tot}(z)$ of the total passive suspension. Here the reaction body force $-f_z^p(z) = 0$, and hence the solvent pressure $P_s(z)$ is constant, as argued before. It is only due to the bulk colloid pressure $P(z_b) = \rho k_B T$ that the total bulk pressure $P_{tot}(z_b)$ is higher than the total reservoir pressure $P_{tot}(z_{res})$. The osmotic pressure $\Pi = P_{tot}(z_b) - P_{tot}(z_{res})$ is therefore equal to $\rho k_B T$. The profiles for an active system ($Pe = 3$), displayed in Fig. 3(d), show that the solvent bulk pressure $P_s(z_b)$ exceeds the solvent reservoir pressure $P_s(z_{res})$. This is caused by the reaction body force $-f_z^p(z)$, that pushes solvent towards the bulk, as pictured in Fig. 1(b). As a result, both the total bulk pressure $P_{tot}(z_b)$ and the osmotic pressure Π exceed their passive counterparts by $\Delta P_s = \gamma_t \gamma_r v_0^2 / 6 k_B T$ on account of eqn (6) for the torque-free potential of interest here.

Fig. 3 (a) External potential $V(z)$ modelling the planar membrane of Fig. 1 that separates the reservoir at $z_{res} = -4\ell$ from the bulk suspension at $z_b = 3\ell$. (b) The steady state propulsion body force $f_z^p(z)$, at activity Pe. Passive (c) and active (d) pressure profiles of the colloids $P(z)$, the solvent $P_s(z)$, and the total suspension $P_{tot}(z) = P(z) + P_s(z)$. For the passive system ($Pe = 0$), $P_s(z)$ is constant, such that the osmotic pressure $\Pi = P_{tot}(z_b) - P_{tot}(z_{res})$ equals the bulk colloid pressure $P(z_b) = \rho k_B T$. For the active system ($Pe = 3$), the reaction body force $-f_z^p(z)$ increases the bulk solvent pressure $P_s(z_b)$, as well as $P_{tot}(z_b)$ and Π, by ΔP_s.

Experimental predictions

The experiments that have addressed the pressure of active systems[38,47,53] are few in number. In particular, the osmotic pressure has never been measured directly. Despite the simplicity of the ABP model, that neglects e.g. hydrodynamic interactions, our expression for the osmotic pressure does allow to estimate the order of magnitude of the meniscus height difference $H = \Pi/(\rho_s^m g)$ that is to be expected in the experiment sketched in Fig. 1. Here we focus on an aqueous dispersion (mass density $\rho_s^m = 1$ kg dm^{-3}) of active hard spheres of radius a, with friction coefficients given by the Stokes relations $\gamma_t = 6\pi\eta a$ and $\gamma_r = 8\pi\eta a^3$, subject to Earth's gravitational acceleration g, at room temperature, and at packing fraction 0.01 that should mimic the ideal (non-interaction) conditions. The predicted height differences H are shown in Fig. 4(a). Whereas the passive osmotic pressure $\rho k_B T$ induces a passive rise $H_0 \sim a^{-3}$ too small to measure for colloidal particles, activity induces an additional rise $\Delta H \sim \Delta P_s \sim a v_0^2$ that brings $H = H_0 + \Delta H$ up to the regime of micrometers[65,70,71] or even millimeters[64] for the larger values of propulsion speed v_0 and particle size a of experimentally realized microswimmers.

To determine experimentally that the activity-induced increase in osmotic pressure results from the increase in solvent pressure ΔP_s, we propose to confine active particles by
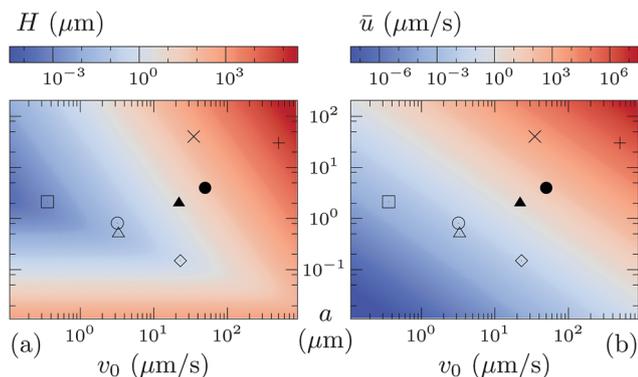
Fig. 4 (a) Predicted rise $H = H_0 + \Delta H$ in Fig. 1, for spherical particles of radius a at propulsion speed v_0 at packing fraction 0.01 in water. (b) Predicted mean solvent velocity $\bar{u}$ in Fig. 2, for a cylindrical pipe of radius $5a$ and length $100a$. Symbols denote literature values of (v_0,a) combinations of experimentally realized self-propelled colloids +,[64] ×,[65] ◇,[66] ○,[67] △,[68] □;[69] and motile bacteria ●,[70] ▲.[71]

a membrane to one half of an open, horizontal pipe, for which gravity plays no role, as illustrated in Fig. 2. Applying equal solvent pressures to either side of the pipe, rather than the no-flux boundary condition before, results in a steady state where the reaction body force near the membrane $-\mathbf{f}^p$ drives a steady solvent flow $\mathbf{u}(\mathbf{r})$ through the pipe (as seen in the lab frame), according to eqn (5). In the limit $|\mathbf{u}(\mathbf{r})| \ll v_0$, and for a cylindrical pipe, this flow velocity is identical to the Poiseuille flow that would be generated in a pipe filled with only solvent upon applying the solvent pressure difference ΔP_s of eqn (6) between either end of the pipe. For a derivation see Section 6 of the ESI.† The predicted mean solvent velocity $\bar{u} \sim a^2 v_0^2$ is shown in Fig. 4(b) as a function of the propulsion speed v_0 and colloid radius a, for a pipe of radius $5a$ and length $100a$. For the larger values of v_0 and a of experimentally realized swimmers,[64,65,70,71] the solvent velocity $\bar{u}$ (although not satisfying $\bar{u} \ll v_0$ in all cases) is predicted to be on the order of micrometers per second, and hence easily detectable, e.g. by using tracer particles.

The solvent chemical potential

We now return to the original setting of Fig. 1 to interpret the solvent pressure difference ΔP_s between the suspension and the reservoir. Even though the active suspension is out of equilibrium, the solvent pressure $P_s(z)$ can still be used to define a meaningful intrinsic solvent chemical potential $\mu_s^{\text{int}}(z)$ by the (Gibbs–Duhem like) relation $\rho_s(z)\partial_z\mu_s^{\text{int}}(z) = \partial_z P_s(z)$, with $\rho_s(z)$ the number density of the solvent (see Section 3 of the ESI† for details). Hence, the solvent pressure difference ΔP_s is accompanied by a difference in the intrinsic solvent chemical potential

$$\Delta\mu_s \equiv \mu_s^{\text{int}}(z_b) - \mu_s^{\text{int}}(z_{\text{res}}) = \int_{z_{\text{res}}}^{z_b} dz \frac{\partial_z P_s(z)}{\rho_s(z)}. \qquad (9)$$

We can thus rephrase our findings as follows. Activity increases the solvent chemical potential of the bulk suspension from the

reservoir value μ_s to $\mu_s + \Delta\mu_s$. The total bulk pressure $P_{\text{tot}}(\rho,\mu_s + \Delta\mu_s) = \rho k_B T + P_s(\mu_s + \Delta\mu_s)$ increases accordingly, such that the osmotic pressure $\Pi = P_{\text{tot}}(\rho,\mu_s + \Delta\mu_s) - P_s(\mu_s)$, which is the difference between the total bulk pressure and the reservoir pressure, now equals $\Pi = \rho k_B T + \Delta P_s$, where $\Delta P_s = P_s(\mu_s + \Delta\mu_s) - P_s(\mu_s)$ is the difference in solvent pressures accompanying the difference in solvent chemical potentials.

In this light, we address the second term of eqn (6), present for anisotropic colloids experiencing a torque $-\partial_\theta V(z,\theta)$. To investigate the implications of this term, we have solved the Smoluchowski eqn (1) for active dumbells, consisting of two point particles with separation $\ell = (\gamma_r/\gamma_t)^{1/2}$. Both point particles are subject to the same membrane potential $V(z) = \lambda k_B T(z/\ell)^2$ for $z < 0$ as before, where the strength parameter λ can now be varied. The resulting potential acting on a dumbell, $V(z,\theta) = V\left(z + \frac{\ell}{2}\cos\theta\right) + V\left(z - \frac{\ell}{2}\cos\theta\right)$, exerts a nonzero torque $-\partial_\theta V(z,\theta)$, that tends to align dumbells parallel to the wall. Fig. 5 shows the resulting increase in solvent pressure ΔP_s, calculated from eqn (6), for different activities Pe as a function of the strength λ of the colloid–membrane interaction potential. For Pe > 0, ΔP_s decreases with λ. The reason for this decrease is that the torque generated by the potential rotates the particles that propel 'into' the membrane, and thereby influences the shape of the polarization profile $m_z(z)$. As it turns out, the torque reduces the total polarization near the membrane $-\int_{z_{\text{res}}}^{z_b} dz m_z(z)$, and by that also the integrated reaction body force $-\int_{z_{\text{res}}}^{z_b} dz f_z^p(z)$ that pushes solvent towards the suspension, see eqn (4). Consequently, the increase in solvent pressure decreases as the strength of the colloid–membrane interaction potential increases. The same dependence was found in ref. 33 for ellipsoidal particles under the assumptions that the distribution attains its bulk value already at $z = 0$, and that the effect of ellipses that only feel the potential partially is negligible. We thus confirm the conclusion of ref. 33 that the second term of eqn (6) depends on the precise form of the colloid–membrane interaction potential $V(z,\theta)$, by a numerical solution $\psi(z,\theta)$ that does not require any further assumptions.

Whereas in ref. 33 this finding was reason to question whether the osmotic pressure is a state function, we emphasize it is the bulk state of the suspension itself that depends on the
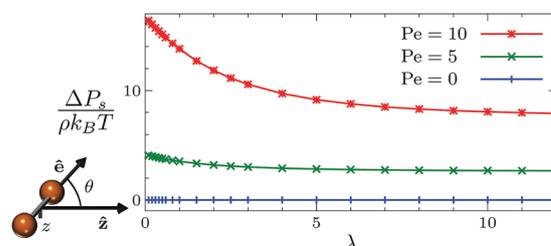

Fig. 5 Increase in bulk solvent pressure ΔP_s as a function of the strength λ of the soft colloid–membrane interaction potential in the setting of Fig. 1 for active dumbells at varying activity Pe. For active systems (Pe > 0), ΔP_s depends on λ.

colloid–membrane potential. To appreciate its consequences, we note that in equilibrium the ensemble of reservoir *and* suspension is specified by the state variables (μ_s, ρ, T), since the solvent chemical potential of the reservoir sets the same chemical potential in the suspension. The fact that for an active system the solvent pressure difference ΔP_s – and thereby also the chemical potential difference $\Delta \mu_s$ – generally depends on the colloid–membrane interaction potential, implies that a complete specification of the ensemble requires an additional state variable, *e.g.* the bulk solvent chemical potential $\mu_s^b \equiv \mu_s + \Delta \mu_s$. In fact, upon including effective colloid–colloid interactions, the activity is also required as a state variable, *e.g.* in terms of v_0 (see Section 3 of the ESI†). A complete set of (intensive) state variables therefore reads $(\mu_s, \mu_s^b, \rho, T, v_0)$. All the mentioned pressures, including the osmotic pressure, *are* state functions of these variables.

Conclusions

We have generalized Van't Hoff's law to active suspensions. We have shown that the active particles exert a net reaction force on the solvent, an effect that we predict to be experimentally measurable either as a solvent flow through a semipermeable membrane confining the active suspension to one side of an open pipe, or as a macroscopic rise of the suspension meniscus in a *U*-pipe experiment. In the latter case, the reaction force increases the solvent pressure of the suspension, and thereby the solvent chemical potential. Remarkably, this increase, and thereby the bulk state of the suspension itself, depends on the details of the colloid–membrane interactions. The osmotic pressure *is* a state function of (amongst others) the solvent chemical potential; it *does* depend on the details of the colloid–membrane interactions, but only *via* the solvent chemical potential.

Discussion

The predictions of eqn (6) and of Fig. 4 are made for active particles whose orientation changes only by rotational diffusion with a rate that follows from the Stokes–Einstein relations for spherical particles. The corresponding typical reorientation time τ_r, equal to $\gamma_r/k_B T$ in this case, is shown by eqn (6) to be proportional to the excess solvent pressure ΔP_s. In fact, the result $\Delta P_s \sim \tau_r$ is more general,[36] because the typical time τ_r that a particle spends propelling 'into' the membrane determines the magnitude of the time-averaged reaction force it exerts on the solvent, and thus of the excess solvent pressure ΔP_s. In general, this reorientation time τ_r depends on more factors, for instance on the details of the propulsion mechanism of the active particle, and on its (hydrodynamic) interaction with the membrane.[59,72] An interesting example of the latter type occurs for the square-shaped particles simulated in ref. 73. These particles tend to form a crystal phase next to the membrane, with the majority of particles facing the membrane.[74] This effect increases τ_r, and thereby the excess solvent pressure ΔP_s, dramatically.

In the ESI,† we generalize the framework presented here to include interactions. The active version of Van't Hoff's law (8) then generalizes to $\Pi = P(\rho, \mu_s^b, v_0) + \Delta P_s$, where $P(\rho, \mu_s^b, v_0)$ now denotes the full pressure (ideal gas plus virial contributions) of the effective colloids-only system that is characterized by (ρ, μ_s^b, v_0). Hence, the functional form of the osmotic pressure Π differs from its passive expression only by the excess solvent pressure ΔP_s. This excess pressure ΔP_s again depends on the membrane potential, except in the absence of any torque inter-actions between either the particles and the membrane, or between the particles themselves. In the absence of such torques, ΔP_s again reduces to the known swim pressure. While this swim pressure is a linear function of ρ at low colloid densities, *cf.* eqn (6), it typically becomes a decreasing function of ρ at high densities.[27,34,39,75] For general interactions, it remains true that the difference in solvent pressure ΔP_s is accompanied by a difference in solvent chemical potential $\Delta \mu_s$, and that the osmotic pressure is a state function of the variables $(\mu_s, \mu_s^b, \rho, T, v_0)$.

Crucial in our approach is that activity enters the colloid force balance (3) as the body force $\mathbf{f}^p(\mathbf{r})$, *cf.* ref. 41, whereas the local pressure $P(\mathbf{r}) = \rho(\mathbf{r})k_B T$ is of the same form as in equilibrium. Our approach follows Speck and Jack,[46] who showed that the bulk colloid pressure represents momentum flux of non-interacting colloids. In the interacting case, the local pressure tensor genera-lizes to a local pressure tensor, that consists of both momentum flux and a term accounting for interaction forces (see Section 1 of the ESI†), as the conventional local pressure tensor does.[76] Representing activity by a body force contrasts the approach of some authors who account for activity, in a colloid-only picture, by modifying the local pressure.[25,32,43,50] Whereas our approach is valid for general particle–particle and particle–wall interactions, this 'activity-modified' local pressure has only been defined for isotropic particles, and indeed its derivation[51,77] does not seem to be extendable to systems with torque interactions.

The generalizations of the force balances (3), (5) and (7) to an interacting suspension (see Section 3 of the ESI†) can readily be applied to other typical phenomena exhibited by active systems, such as the motility-induced phase separation (MIPS) of purely repulsive particles.[11,12,15,78,79] Strikingly, the interface of the phase coexistence generated by MIPS was found to have a negative interfacial tension, defined in the colloid-only picture in terms of the activity-modified pressure tensor.[43] This begs the question what this negative interfacial tension – and its inter-pretation[43,80] – translates into in the picture presented here, both in the colloid-only sense and upon taking the solvent into account.

We foresee the picture presented here to form a basis for making headway in understanding this extraordinary world of active matter physics, and express the hope that the predictions of Fig. 4 will stimulate experimental efforts to actually measure the osmotic pressure and the associated solvent pressure difference ΔP_s of active suspensions.

Conflicts of interest

There are no conflicts of interest to declare.

Acknowledgements

References

1 J. van't Hoff, *Z. Phys. Chem.*, 1887, **1**, 481.
2 J. van't Hoff, *Philos. Mag.*, 1888, **26**, 81.
3 J. van't Hoff, in *The Role of Osmotic Pressure in the Analogy between Solutions and Gases*, ed. H. C. Jones, Harper & Brothers Publishers, New York and London, 1899, p. 11.
4 H. C. Berg, *E. coli in Motion*, Springer, 2003.
5 J. Schwarz-Linek, J. Arlt, A. Jepson, A. Dawson, T. Vissers, D. Miroli, T. Pilizota, V. A. Martinez and W. C. K. Poon, *Colloids Surf., B*, 2016, **137**, 2.
6 S. J. Ebbens and J. R. Howse, *Soft Matter*, 2010, **6**, 726.
7 H. H. Wensink, V. Kantsler, R. E. Goldstein and J. Dunkel, *Phys. Rev. E: Stat., Nonlinear, Soft Matter Phys.*, 2014, **89**, 010302.
8 V. Prymidis, H. Sielcken and L. Filion, *Soft Matter*, 2015, **21**, 4158.
9 A. Snezhko and I. S. Aranson, *Nat. Mater.*, 2011, **10**, 698.
10 L. Baraban, M. Tasinkevych, M. N. Popescu, S. Sanchez, S. Dietrich and O. G. Schmidt, *Soft Matter*, 2012, **8**, 48.
11 M. E. Cates and J. Tailleur, *Annu. Rev. Condens. Matter Phys.*, 2015, **6**, 219.
12 M. C. Marchetti, Y. Fily, S. Henkes, A. Patch and D. Yllanes, *Curr. Opin. Colloid Interface Sci.*, 2016, **21**, 34.
13 I. Theurkauff, C. Cottin-Bizonne, J. Palacci, C. Ybert and L. Bocquet, *Phys. Rev. Lett.*, 2012, **108**, 268303.
14 J. Palacci, S. Sacanna, A. P. Steinberg, D. J. Pine and P. M. Chaikin, *Science*, 2013, **339**, 936.
15 I. Buttinoni, J. Bialké, F. Kümmel, H. Löwen, C. Bechinger and T. Speck, *Phys. Rev. Lett.*, 2013, **110**, 238301.
16 T. Vicsek, A. Czirók, E. Ben-Jacob, I. Cohen and O. Shochet, *Phys. Rev. Lett.*, 1995, **75**, 1226.
17 Y. Fily and M. C. Marchetti, *Phys. Rev. Lett.*, 2012, **108**, 235702.
18 G. S. Redner, A. Baskaran and M. F. Hagan, *Phys. Rev. E: Stat., Nonlinear, Soft Matter Phys.*, 2013, **88**, 012305.
19 J. Bialké, H. Löwen and T. Speck, *Europhys. Lett.*, 2013, **103**, 30008.
20 A. Wysocki, R. G. Winkler and G. Gompper, *Europhys. Lett.*, 2014, **105**, 48004.
21 T. Speck, J. Bialké, A. M. Menzel and H. Löwen, *Phys. Rev. Lett.*, 2014, **112**, 218304.
22 S. C. Takatori and J. F. Brady, *Phys. Rev. E: Stat., Nonlinear, Soft Matter Phys.*, 2015, **91**, 032117.
23 T. F. F. Farage, P. Krinninger and J. M. Brader, *Phys. Rev. E: Stat., Nonlinear, Soft Matter Phys.*, 2015, **91**, 042310.
24 S. C. Takatori and J. F. Brady, *Soft Matter*, 2015, **11**, 7920.
25 U. M. B. Marconi and C. Maggi, *Soft Matter*, 2015, **11**, 8768.

26 A. Tiribocchi, R. Wittkowski, D. Marenduzzo and M. E. Cates, *Phys. Rev. Lett.*, 2015, **115**, 188302.
27 S. C. Takatori and J. F. Brady, *Curr. Opin. Colloid Interface Sci.*, 2016, **21**, 24.
28 C. Nardini, E. Fodor, E. Tjhung, F. van Wijland, J. Tailleur and M. E. Cates, *Phys. Rev. X*, 2017, **7**, 021007.
29 M. Dijkstra, S. Paliwal, J. Rodenburg and R. van Roij, 2016, arXiv:1609.02773.
30 A. P. Solon, J. Stenhammar, M. E. Cates, Y. Kafri and J. Tailleur, 2016, arXiv:1609.03483.
31 R. Wittman, C. Maggi, A. Sharma, A. Scacchi, J. M. Brader and U. M. B. Marconi, 2017, arXiv:1701.09032.
32 B. van der Meer, V. Prymidis, M. Dijkstra and L. Filion, 2017, arXiv:1609.03867.
33 A. P. Solon, Y. Fily, A. Baskaran, M. E. Cates, Y. Kafri, M. Kardar and J. Tailleur, *Nat. Phys.*, 2015, **11**, 673–678.
34 X. Yang, M. L. Manning and M. C. Marchetti, *Soft Matter*, 2014, **10**, 6477.
35 R. Wittkowski, A. Tiribocchi, J. Stenhammar, R. J. Allen, D. Marenduzzo and M. E. Cates, *Nat. Commun.*, 2014, **5**, 4351.
36 S. C. Takatori, W. Yan and J. F. Brady, *Phys. Rev. Lett.*, 2014, **113**, 028103.
37 S. C. Takatori and J. F. Brady, *Soft Matter*, 2014, **10**, 9433.
38 F. Ginot, I. Theurkauff, D. Levis, C. Ybert, L. Bocquet, L. Berthier and C. Cottin-Bizonne, *Phys. Rev. X*, 2015, **5**, 011004.
39 A. P. Solon, J. Stenhammar, R. Wittkowski, M. Kardar, Y. Kafri, M. E. Cates and J. Tailleur, *Phys. Rev. Lett.*, 2015, **114**, 198301.
40 C. Maggi, U. M. B. Marconi, N. Gnan and R. D. Leonardo, *Sci. Rep.*, 2015, **5**, 10742.
41 W. Yan and J. F. Brady, *Soft Matter*, 2015, **11**, 6235.
42 R. G. Winkler, A. Wysocki and G. Gompper, *Soft Matter*, 2014, **11**, 6680.
43 J. Bialké, J. T. Siebert, H. Löwen and T. Speck, *Phys. Rev. Lett.*, 2015, **115**, 098301.
44 W. Yan and J. F. Brady, *J. Fluid Mech.*, 2015, **785**, R1.
45 M. Joyeux and E. Bertin, *Phys. Rev. E*, 2016, **93**, 032605.
46 T. Speck and R. L. Jack, *Phys. Rev. E*, 2016, **93**, 062605.
47 S. C. Takatori, R. D. Dier, J. Vermant and J. F. Brady, *Nat. Commun.*, 2016, **7**, 10694.
48 N. Nikola, A. P. Solon, Y. Kafri, M. Kardar, J. Tailleur and R. Voituriez, *Phys. Rev. Lett.*, 2016, **117**, 098001.
49 G. Falasco, F. Baldovin, K. Kroy and M. Baiesi, *New J. Phys.*, 2016, **18**, 093043.
50 J. Blaschke, M. Maurer, K. Menon, A. Zöttl and H. Stark, *Soft Matter*, 2016, **12**, 9821.
51 S. Steffenoni, G. Falasco and K. Kroy, *Phys. Rev. E*, 2017, **95**, 052142.
52 D. Levis, J. Codina and I. Pagonabarraga, 2017, arXiv:1703.02412.
53 G. Junot, G. Briand, R. Ledesma-Alonso and O. Dauchot, *Phys. Rev. Lett.*, 2017, **119**, 028002.
54 S. C. Takatori and J. F. Brady, 2017, arXiv:1709.05461.
55 T. W. Lion and R. J. Allen, *Europhys. Lett.*, 2014, **106**, 34003.

56 M. C. Marchetti, J. F. Joanny, S. Ramaswamy, T. B. Liverpool, J. Prost, M. Rao and R. A. Simha, *Rev. Mod. Phys.*, 2013, **85**, 1143–1189.

57 P. Romanczuk, M. Bär, W. Ebeling and B. Lindner, *Eur. Phys. J.: Spec. Top.*, 2012, **202**, 1.

58 L. Rothschild, *Nature*, 1963, **198**, 1221.

59 A. P. Berke, L. Turner, H. C. Berg and E. Lauga, *Phys. Rev. Lett.*, 2008, **101**, 038102.

60 G. Li and J. X. Tang, *Phys. Rev. Lett.*, 2009, **103**, 078101.

61 J. Elgeti and G. Gompper, *Europhys. Lett.*, 2013, **101**, 48003.

62 C. Lee, *New J. Phys.*, 2013, **15**, 055007.

63 Y. Fily, A. Baskaran and M. F. Hagan, *Phys. Rev. E: Stat., Nonlinear, Soft Matter Phys.*, 2015, **91**, 012125.

64 P. G. Moerman, H. W. Moyses, E. B. van der Wee, D. G. Grier, A. van Blaaderen, W. K. Kegel, J. Groenewold and J. Brujic, *Phys. Rev. E*, 2017, **96**, 032607.

65 J. Vicario, R. Eelkema, W. R. Browne, A. Meetsma, R. M. L. Crois and B. L. Feringa, *Chem. Commun.*, 2005, 3936.

66 D. A. Wilson, R. J. M. Nolte and J. C. M. van Hest, *Nat. Chem.*, 2012, **4**, 212.

67 J. R. Howse, R. A. L. Jones, A. J. Ryan, T. Gough, R. Vafabakhsh and R. Golestanian, *Phys. Rev. Lett.*, 2007, **99**, 048102.

68 J. Palacci, C. Cottin-Bizonne, C. Ybert and L. Bocquet, *Phys. Rev. Lett.*, 2010, **105**, 088304.

69 G. Volpe, I. Buttinoni, D. Vogt, H. Kümmerer and C. Bechinger, *Soft Matter*, 2011, **7**, 8810.

70 M. Mussler, S. Rafa, P. Peyla and C. Wagner, *Europhys. Lett.*, 2013, **101**, 54004.

71 K. Drescher, J. Dunkel, L. H. Cisneros, S. Ganguly and R. E. Goldstein, *Proc. Natl. Acad. Sci. U. S. A.*, 2011, **108**, 10940.

72 E. Lauga, W. R. DiLuzio, G. M. Whitesides and H. A. Stone, *Biophys. J.*, 2006, **90**, 400.

73 V. Prymidis, S. Samin and L. Filion, *Soft Matter*, 2016, **12**, 4309.

74 V. Prymidis, private communication, 2017.

75 V. Prymidis, S. Paliwal, M. Dijkstra and L. Filion, *J. Chem. Phys.*, 2016, **145**, 124904.

76 J. S. Rowlinson and B. Widom, *Molecular Theory of Capillarity*, Dover Publications, 1982.

77 Y. Fily, Y. Kafri, A. Solon, J. Tailleur and A. Turner, 2017, arXiv:1704.06499.

78 A. Zöttl and H. Stark, *Phys. Rev. Lett.*, 2014, **112**, 118101.

79 R. Matas-Navarro, R. Golestanian, T. B. Liverpool and S. M. Fielding, *Phys. Rev. E: Stat., Nonlinear, Soft Matter Phys.*, 2014, **90**, 032304.

80 T. Speck, *Europhys. Lett.*, 2016, **114**, 30006.